Behaviour of Three Test Embankments Taken to Failure on Soft Clay

M.S.S. Almeida, H.M. Oliveira, D. Dias, L.O.G. Deotti

Abstract. This article compares and analyses the behaviour of three test embankments. The soil foundation consisted of normally consolidated clay overlain by a thick sand surface layer. The embankments were rapidly constructed until failure, which occurred after approximately 50 days. Two of the embankments were reinforced, one including prefabricated vertical drains (PVD), while the third had neither reinforcement nor PVDs. The two reinforced embankments presented similar net embankment heights (fill thickness minus average settlement) at failure, owing to the similarity in the undrained strength values of the two clay layers. The test embankment with PVDs showed that this drainage feature improved overall behaviour but the benefit was less than suggested in the literature, owing to the low coefficient of consolidation of the normally consolidated clay, rapid construction and drain disturbance effects. Numerical analyses of the test embankment with PVDs showed good overall agreement between measured and computed values and confirmed overall field observations. The embankment without reinforcement and PVDs reached a greater embankment height than the two reinforced embankments, owing to its greater clay strength.

Keywords: displacements, embankment, pore pressure, soft clay, vertical drains, numerical analyses.

1. Introduction

The construction of embankments on very soft soils requires careful control of settlement and stability (Bergado *et al.*, 1994; Rowe & Leroueil, 2001). Prefabricated vertical drains (PVD) are commonly adopted for the acceleration of settlement by providing short horizontal drainage paths (Holtz, 1987; Almeida *et al.*, 2001, Almeida *et al.*, 2005; Lo *et al.*, 2008) and geosynthetic reinforcement (Humphrey & Holtz, 1989; Rowe *et al.*, 1995, 1996; Chai *et al.*, 2002; Kelln *et al.*, 2007) has been used to improve the stability of these soil structures. The combined use of PVDs and geosynthetic reinforcement may allow for higher embankments and short construction times in comparison with conventional construction methods (*e.g.*, Li & Rowe, 2001; Rowe & Li, 2005). Most of the literature studies are related to embankments placed directly on soft clays or placed on top of shallow surface sand layers, which is not the present case.

This article compares the behaviour of three instrumented test embankments constructed until failure on normally consolidated very soft clay layers overlain by working platforms 1.7 to 2.1 m thick. Usually, working platforms are constructed immediately before the actual embankment but in the present case they were constructed six years before embankment construction. Two of the embankments were reinforced, one had PVDs and the other did not have PVDs. A third embankment was constructed without reinforcement and without PVDs.

Horizontal and vertical displacements and pore pressure measurements are presented and compared. The three embankments were loaded until foundation failure occurred also for the reinforced embankments as failure of the reinforcement did not take place. Numerical analyses of the test embankment provided with PVDs were also carried out to clarify the influence of the PVDs on short term construction to failure.

2. The Test Embankments

The test embankments and the motorway are located on Santa Catarina Island in the city of Florianópolis, on the southern coast of Brazil, as shown in Fig. 1. In the southern part of the island, a very soft clay deposit 4 to 22 m thick is found.

Around 1996 a sand hydraulic fill was constructed in a bay where the motorway was planned to pass in order to raise the ground level above sea level, because the area used to be flooded at various times during the year. Although the surface sand layer generally worked well, a number of failures occurred. As a result, three test embankments, TE1, TE2 and TE3, were planned and completed (Magnani, 2006) by late 2002 on the Florianópolis clay, with the aim

M.S.S. Almeida, Ph.D., Graduate School of Engineering, COPPE, Universidade Federal do Rio de Janeiro, Caixa Postal 68506, 21945 Rio de Janeiro, RJ, Brazil. e-mail: almeida@coc.ufrj.br.
H.M. Oliveira, D.Sc., Departamento de Engenharia Civil, Universidade Federal de Santa Catarina, Rua João Pio Duarte da Silva 205, 88040-970 Carrego Grande, Florianópolis, SC, Brazil. e-mail: henriquemagnani@uol.com.br.
D. Dias, D.Sc., LTHE Laboratory, Joseph-Fourier University, UMR 5564 bp 53, 38041 Grenoble, France. e-mail: daniel.dias@ujf-grenoble.fr.
L.O.G. Deotti, M.Sc., COPPE, Universidade Federal do Rio de Janeiro and ELETROBRAS, Rua do Ouvidor 107, 20040-031 Centro, Rio de Janeiro, R.J., Brazil. e-mail: leodeotti@hotmail.com; lguerra@eletrobras.com.
Submitted on February 6, 2012; Final Acceptance on December 15, 2011; Discussion open until July 31, 2012.

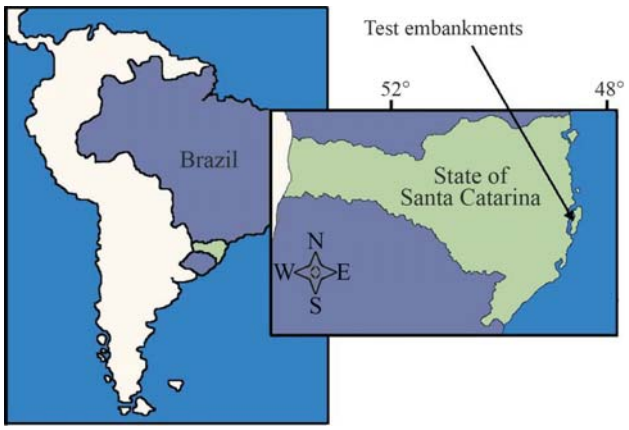

Figure 1 - Location of the test embankments.

of providing relevant data for the construction of the motorway. The motorway embankment would have a thick sand surface layer and be reinforced and provided with PVDs in the clay layer. Therefore, it was decided that the three test embankments should be constructed in areas with pre-existing surface sand layers. Embankments TE1 and TE2 were provided with 200 kN/m x 45 kN/m Stabilenka® polyester reinforcement with a modulus $J_{5\%}$ = 1700 kN/m for 5% strain. Prefabricated Colbonddrain® CX 1000 drains (10 cm x 0.5 cm) in a triangular mesh with 1.30 m spacing were placed in section TE1. Embankment TE3 was constructed without reinforcement and PVDs. The test embankments were raised until failure occurred after around 50 days.

The three test embankments had essentially the same geometry and instrumentation, although their foundations had different clay thicknesses, as explained below. Figure 2 shows the geometry and instrumentation used in embankment TE1. The transverse section of embankment TE1 (before and after failure) is shown in Fig. 2a with slopes 1(V): 1.5(H). The three embankments also had the same plan geometry (see Fig. 2b), platform width 20 m by 30 m and lateral berms 1.0 m high and 12 m long aimed at inducing failure in the intended transverse direction. Given that the base of the embankment had a slight inclination, the direction of the failure was naturally defined by this inclination.

The test embankments were instrumented as exemplified in Fig. 2 for embankment TE1. The embankments were monitored in terms of vertical displacements (eight settlement plates; three verticals of magnetic extensometers and three lines, each with six surface marks), horizontal displacements (three vertical inclinometers) and pore pressure (three electric vibrating wire piezometers) near the embankment centre line. Four specially designed load cells (Almeida *et al.*, 2010) were used to measure the tensile force mobilised in the reinforcement. With the exception of the load cell, all the instruments used are commonly applied in geotechnical engineering (Dunnicliff, 1988).

The measured tensile forces in the reinforcement (Magnani *et al.*, 2009) were relatively small in the present case, owing to the existence of the surface sand layer. Measured tensile forces at the two reinforced embankments for failure conditions were in the range 40-50 kN/m but at service state conditions (factor of safety around 1.4) much lower values, of the order of 4 to 7 kN/m, were developed. Stability analyses (Magnani *et al.*, 2010) using tensile forces measured in the reinforcement indicate that the reinforcement made a very small contribution to the increase in the factors of safety, *i.e.*, at failure conditions the reinforcement increased the factors of safety by 2.4% and 3.6% respectively for embankments TE1 and TE2 with respect to the same (hypothetically) unreinforced embankments. Stability analyses also showed that the surface sand layers contributed by increasing the factors of safety by 43% to 60% with respect to the same (hypothetical) embankments without the surface sand layers, unreinforced in both cases.

This article assesses the behaviour until failure of the three embankments with respect to the importance of reinforcement and PVDs, with emphasis on displacement and pore pressure data. The analysis of the forces measured by the reinforcement load cells, discussed in detail by Magnani *et al.* (2009), is outside the scope of this article. The results of stability analyses are also considered for the overall understanding of the performances of the three embankments. Numerical analyses of the embankment provided with PVDs complemented field observations and clarified the importance of the PVDs in the present cases.

3. Foundation Soils and Fill Materials

Geotechnical investigations were carried out under the auspices of the motorway engineering project and included vane and piezocone tests as well as triaxial and consolidation tests. Table 1 summarises the geotechnical characteristics of the Florianopolis clay, obtained from various investigation projects carried out between 1979 and 2002, the later date referring to the year of the test embankment construction. Florianopolis clay is very soft, with low organic content and medium sensitivity. The results of the present investigation are consistent with the behaviour of clays located along the south and south-east coast of Brazil (Almeida & Marques, 2002; Almeida *et al.*, 2008; Massad, 1994; Pinto, 1994).

Figure 3 shows the continuous undrained strength profiles $S_{u(PZ)}$ in the centre of each test embankment obtained from piezocone tests. The $S_{u(PZ)}$ values shown in Fig. 3 make use of the equation:

$$S_{u(PZ)} = \frac{q_T - \sigma_v}{N_{kt}} \quad (1)$$

where q_T is the corrected point resistance measured in piezocone tests, σ_v is the total in situ vertical stress and N_{kt} the empirical cone factor equal to 12.0, as obtained by local correlations between vane and piezocone tests, and which

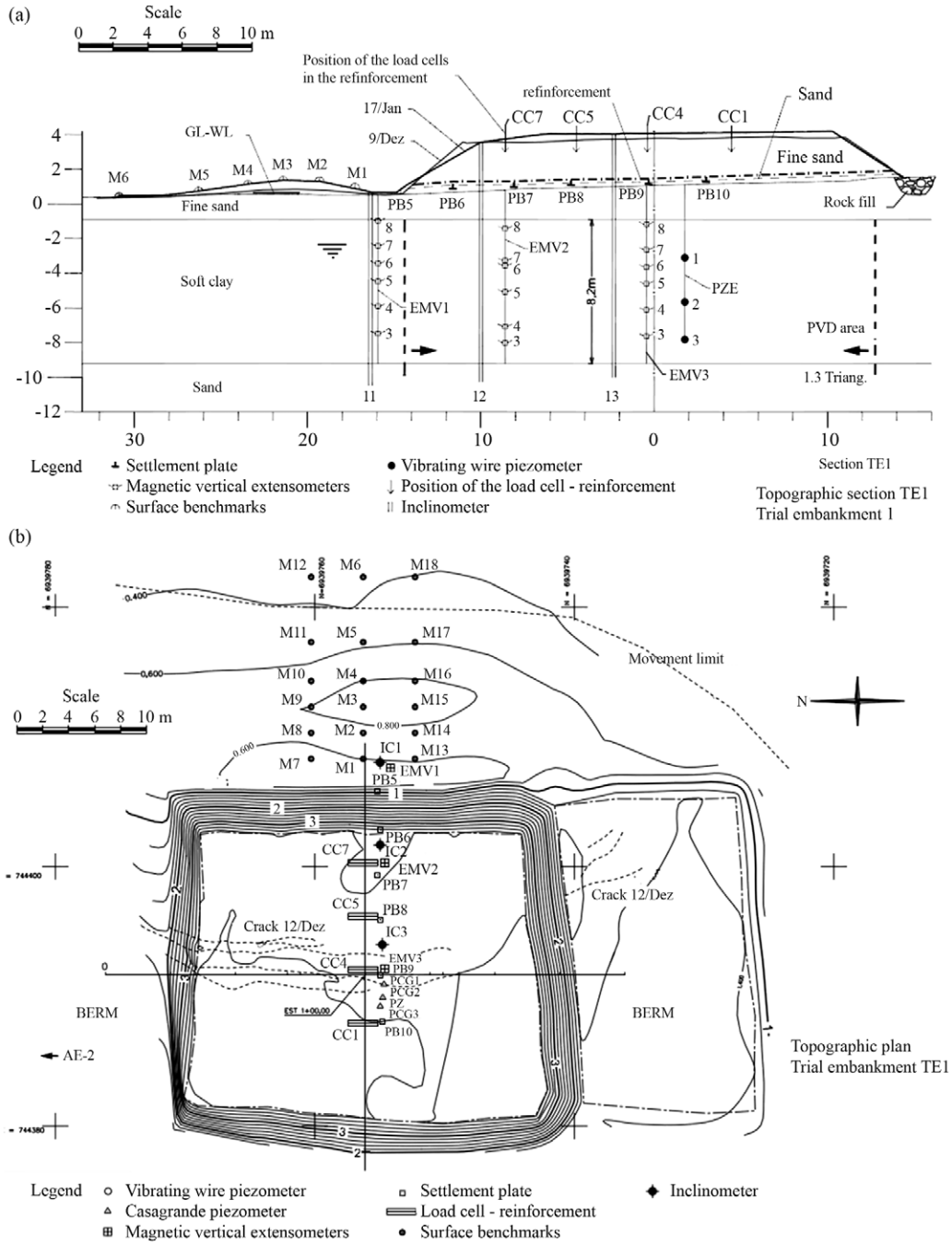

Figure 2 - Test embankment TE-1, with drains and reinforcement: (a) cross-section; (b) plan view.

is also a typical value for Brazilian very soft clays (Schnaid, 2009).

Owing to the local geological variations, the thickness of the soft clay was different for each section of the embankment, as shown in Fig. 3 and Table 2. Thicknesses of the surface sand layer in the three embankments are also indicated in Table 2.

The higher values of S_u measured under embankment TE3 (see Fig. 3) are due to the existence of the sand lens in a less thick clay layer and a thicker surface sand layer acting on the clay surface over a period of six years. Owing to the action of the sand layer surcharge, most of the soft clay layer was close to normally consolidated condition, which was confirmed by oedometer tests and piezocone tests carried out in this clay (Magnani, 2006).

Uniform fine silica sand (95% of the material passing through # 40 sieve and less than 5% passing through # 200 sieve) was used in both the surface sand layer and the embankment. The bulk weight of this sand was $\gamma = 17.5$ kN/m^3, void ratio $e = 0.60$ and degree of saturation $S = 34\%$. Direct

Table 1 - Geotechnical parameters of Florianópolis soft clay.

Parameter	Value
Water content w (%)	100-170
Liquidity index w_L (%)	105-165
Average plasticity index I_p (%)	80
Organic matter content, average percentage in weight (%)	3.8
Bulk weight γ (kN/m^3)	13.2-14.2
Voids ratio e	2.9-4.5
Compression ratio C_c / (1 + e_o)	0.30-0.45
Ratio of compression indices C_s / C_c	0.08-0.14
Vertical coefficient of consolidation c_v - normally consolidated (m^2/s)	0.7-1.0 x 10^{-8}
Vertical coefficient of permeability k_v - (m/s)	1.0 x 10^{-9}
Vane uncorrected undrained strength S_u (kPa)	5-28
Sensitivity (vane)	3-6
Effective friction angle ϕ‘ (degrees)	30.0
Effective cohesion c (kPa)	0.0
Rigidity Index $I_r = G_{50}/S_u$ - obtained from CIU triaxial tests	50
Cone factor N_{kt} (average)	12.0
Pore pressure ratio B_q	0.4-0.6

shear tests indicated a friction angle ϕ = 33.8°. In embankment TE1 with PVDs, a drainage blanket (medium-to-coarse sand) layer with an average thickness of 0.40 m was used.

4. Vertical Displacements

4.1. Vertical displacements at the embankment bases

Vertical displacements at the base of the test embankments were measured by settlement plates under the embankments and surface marks in front of the embankments (see Fig. 2). Figure 4 compares the vertical displacement data for the three embankments and it is noted that the maximum settlement values are closer to the slope than to the central region (embankment axis), particularly in the final loading stages. This sagged pattern of displacements has been found in some embankments (Almeida *et al.*, 1985; Indraratna *et al.*, 1992) and may be attributed to low factors of safety and the shearing yield of the soft clay foundation under the slope (Almeida *et al.*, 1986) as well as to the large width of the embankment compared to its height (Zhang, 1999).

Figure 4 shows that embankment TE1 has the highest settlement values, followed by embankment TE2 and then embankment TE3. Although for the test embankments constructed to failure, the rotational shear movement may control settlements, the fact that the magnitude of settlement is

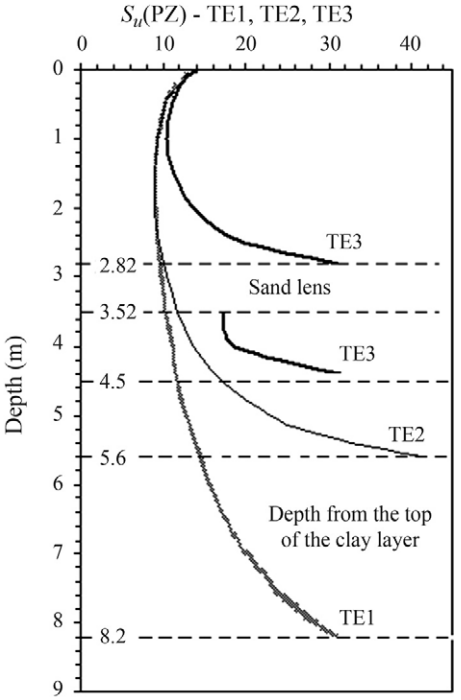

Figure 3 - Undrained strength measured at the three instrumented sections: (a) piezocone S_u profiles (and depth of the clay layers); (b) vane strength S_u *vs.* piezocone measurements.

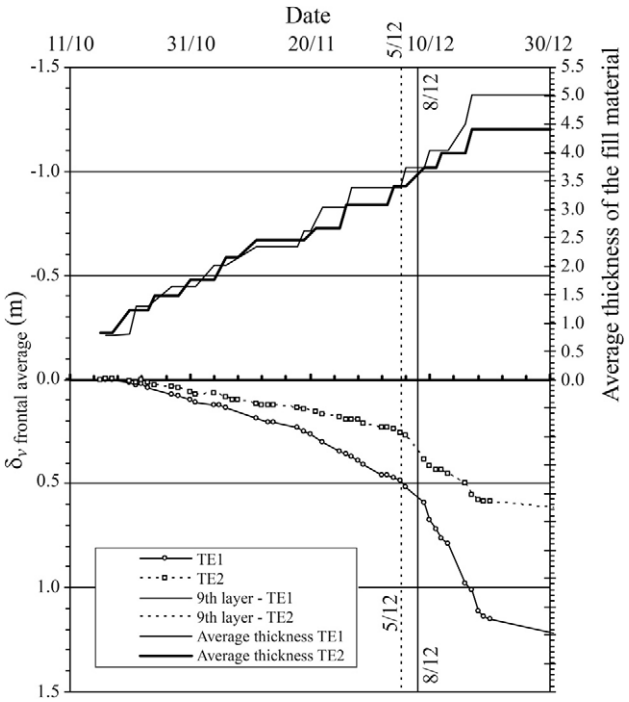

Figure 4 - Vertical displacements of the three test embankments.

proportional to the thickness of the clay layer suggests that consolidation settlements were also relevant in the present case. From the results of the TE2 embankment, the embankment at the centreline was about 0.15 m at the 10th lift

Table 2 - Main features of the three test embankments.

	Embankment		
	TE1	TE2	TE3
Reinforcement	Polyester Stabilenka -200 x 45 kN/m; J = 1700 kN/m		No reinforcement
Vertical drains	Colbondrain CX 1000, 10 cm x 0.5 cm, triangular array, 1.30 m spacing	No drains	No drains
Clay thickness (m)	8.2	5.6	4.5 (sand layer from 2.8 to 3.5 m)
Working platform thickness (sand hydraulic fill) (m)	1.7	1.8	2.1

of the embankment fill, corresponding to 2.7% vertical strain (*i.e.* soft clay thickness was 5.6 m). For the case of TE1 test embankment, whose soft clay foundation thickness was 8.2 m, 2.7% vertical strain would be equal to only 0.22 m of settlement while the field measurements show about 0.5 m of settlement, which implies that more than 55% of the settlement was caused by consolidation. This suggests that PVDs had some effect in accelerating consolidation during construction. This topic is further discussed later in this paper using results of numerical analyses.

4.2. Settlements of the frontal plates

Figure 5 compares vertical settlements δ_v in the four frontal plates (located between the failure surface and frontal slope) of embankments TE1 and TE2. The data shown in Fig. 5 represent the average values of settlement plates PB6, PB7, PB8 and PB9 for embankment TE1 (see Fig. 2) as well as the corresponding data for the four settlement plates for embankment TE2. The instant of the increase in settlement rates indicates the start of the process of embankment failure. This instant is indicated in Fig. 5 by vertical lines and corresponds to the placement of the ninth layer, coincidently for the two embankments. It can be noted that the load histories of the two reinforced embankments were quite similar until failure.

Figure 6 compares the fill thickness *vs.* average frontal settlements for the three embankments. The points corresponding to the onset of failure (first crest cracks) and total collapse are indicated in Fig. 6a. It may be observed that embankment TE3 presents smaller settlements and greater fill thickness compared with embankments TE1 and TE2. The comparison of the two reinforced embankments shows that TE1 presents greater thickness and larger settlements than embankment TE2. These data have also been

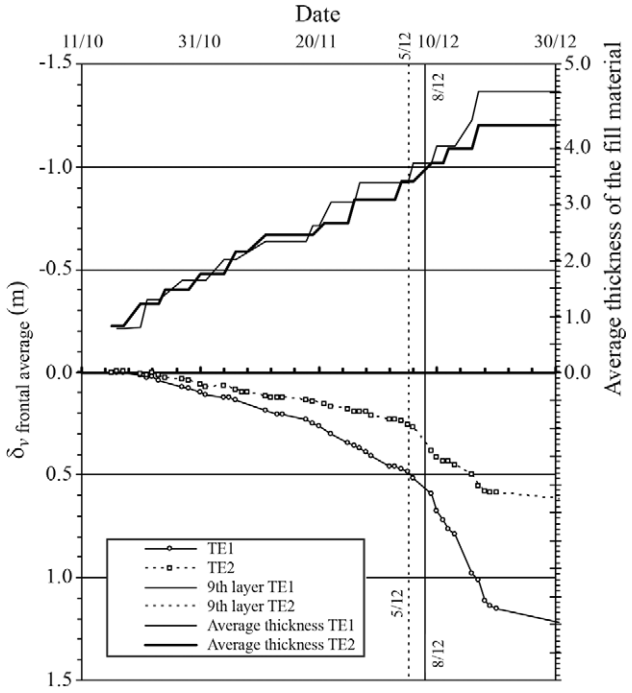

Figure 5 - Average settlement of the frontal settlement plates *vs.* time for embankments TE1 and TE2.

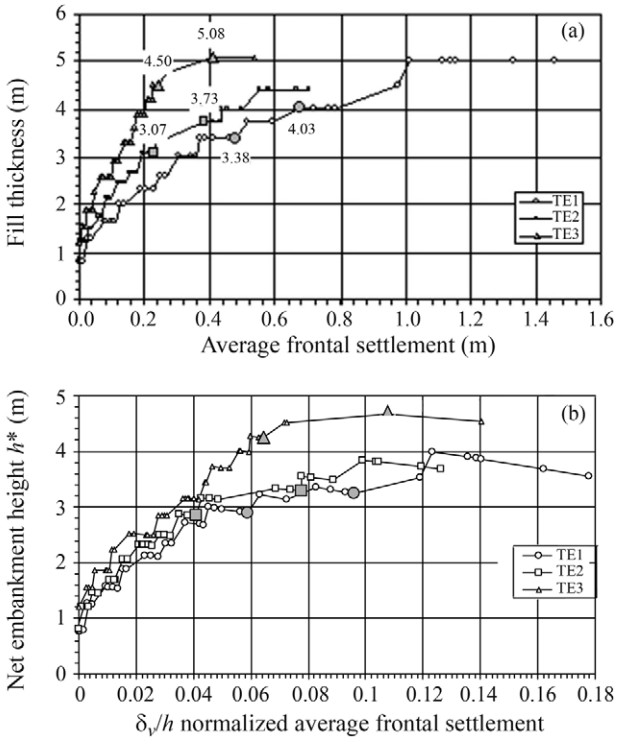

Figure 6 - Average frontal settlement data for embankments TE1, TE2 and TE3.

plotted with respect to net embankment height h^* defined by the embankment thickness minus the average settlement (Rowe & Soderman, 1987; Hinchberger & Rowe, 2003) *vs.* normalised settlement (normalised by the thickness of the clay layer), as shown in Fig. 6b, where the curves of the two reinforced embankments are closer than in Fig. 6a. Thus, the greater thickness in embankment TE1 is compensated by larger settlements and the values of h^* are quite close, particularly at the start of failure and at total collapse. Therefore, the PVDs have increased settlements but not the net embankment height h^*. However, the PVDs may have promoted some gain in strength for two reasons: a) the S_u profile for TE1 showed somewhat lower undrained shear strength than for TE2 (see Fig. 1); b) at failure, both embankments had the same net embankment heights while TE1 had larger settlement (about 0.3 m larger) which means TE1 had higher embankment fill thickness (*i.e.* experienced higher overburden pressure at failure). These two reasons would suggest that PVDs had improved the embankment stability and increased the undrained shear strength of the clay.

It is seen in Fig. 6 that embankment TE3 without reinforcement reaches greater fill thickness and net embankment height than the two reinforced embankments. This is attributed (Magnani, 2006; Magnani *et al.*, 2010) to the greater strength of clay in an undrained state, and also to the presence of the sand lenses under embankment TE3 (see Fig. 3a). For these reasons embankment TE3 may not be considered, in the present cases studied, as a reference unreinforced embankment with respect to the two reinforced embankments.

4.3. Vertical displacements at the embankment toe

The monitoring of vertical displacements at the embankment toe or slightly beyond the toe is an efficient procedure (Hunter & Fell, 2003) to assess the impending failure of embankments on soft clays. Figure 7 shows the results of the vertical magnetic extensometers MTV1 located about 2 m beyond the toe of embankment TE1 (analogous to MTV4 in embankment TE2 – see Fig. 2). It is noted that the extensometers located above the failure surface (indicated by the inclinometers, see item below) experienced upward displacements and the two extensometers located below the failure surface had downward displacements and smaller displacement variations than those above the failure surface.

It can be noted that the displacements of the extensometers closer to the ground surface increased substantially shortly after the placement of the ninth layer, during which cracks at the embankment surface were noted. Data on the frontal plates shown in Fig. 5 support this conclusion. The ninth layer, for that reason, is considered to be the point at which the embankments TE1 and TE2 failed. The results of the inclinometers, discussed at greater length by Magnani *et al.* (2009), support these findings. Similarly, the twelfth layer was considered (Magnani, 2006) to be the moment of failure for the unreinforced embankment TE3.

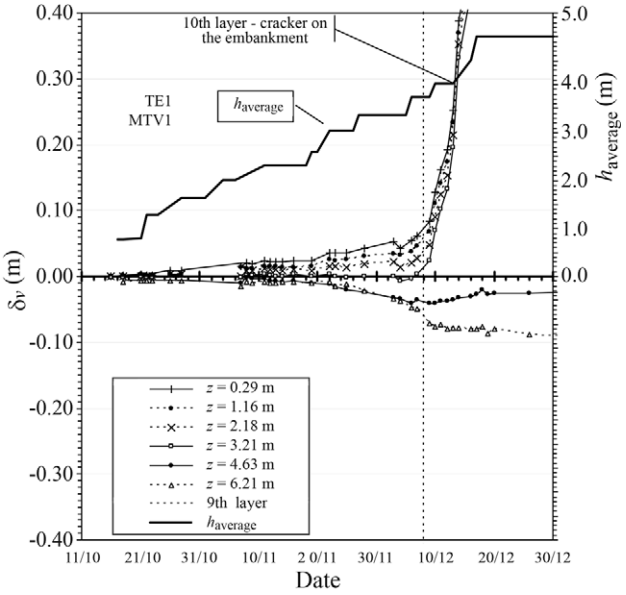

Figure 7 - Vertical displacements measured in vertical extensometers at the embankment toe – test embankment TE1.

5. Central Settlements, Pore Pressure and Consolidation

5.1. Central settlements data

Data on the central settlement plates of embankments TE1 and TE2 with thicker clay layers are analysed here. The three embankments had central plates in similar positions and for TE1 these were PB7, PB8, PB9 and P10, as shown in Fig. 2. These central plates are less influenced by shear-induced settlements and are useful for assessing the consolidation of these two embankments.

Fig. 8 shows the average settlements in the central region normalised by the clay thickness, before failure, plotted against the net applied embankment vertical stress $\Delta\sigma_v$, *i.e.*, the embankment stress less the embankment submergence owing to settlements. Best linear fit lines through the data are also presented. Normalised settlements of embank-

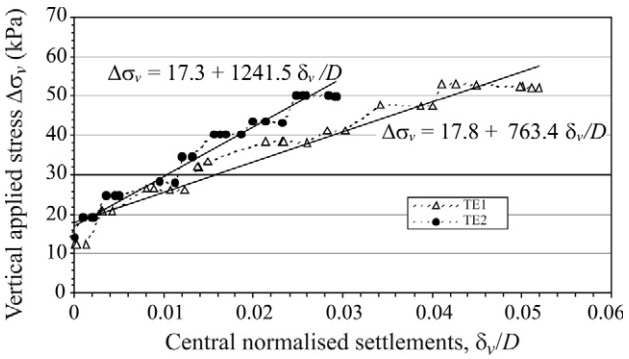

Figure 8 - Central settlements normalised by the clay thickness *vs.* vertical applied stress for embankments TE1 and TE2.

ment TE1 are 1.62 times higher (the ratio between the inclinations of the two best fit lines) than normalised settlements for embankment TE2. TE1 settled more due to its greater clay thickness and the presence of PVDs.

Measured settlements include immediate (undrained) and consolidation settlements. In simple terms, consolidation settlements in Fig. 8 are represented by the settlements under quasi-constant $\Delta\sigma_v$ values and immediate settlements are represented by the settlements owing to the increase in $\Delta\sigma_v$ values; thus the consolidation settlements for embankment TE1 with PVDs in a thicker clay layer are greater than the consolidation settlements for embankment TE2. Despite greater consolidation of embankment TE1 (embankment fill thickness is higher for TE1), however, the net embankment height h^* for embankments TE1 and TE2 was quite similar (see Fig. 6b).

5.2. Excess pore pressures

Measured values of excess pore pressure Δu and the average applied embankment vertical stress $\Delta\sigma_v$ are shown in Fig. 9 for embankments TE1 and TE2. The positions of piezometers under the embankment centre lines are indi-

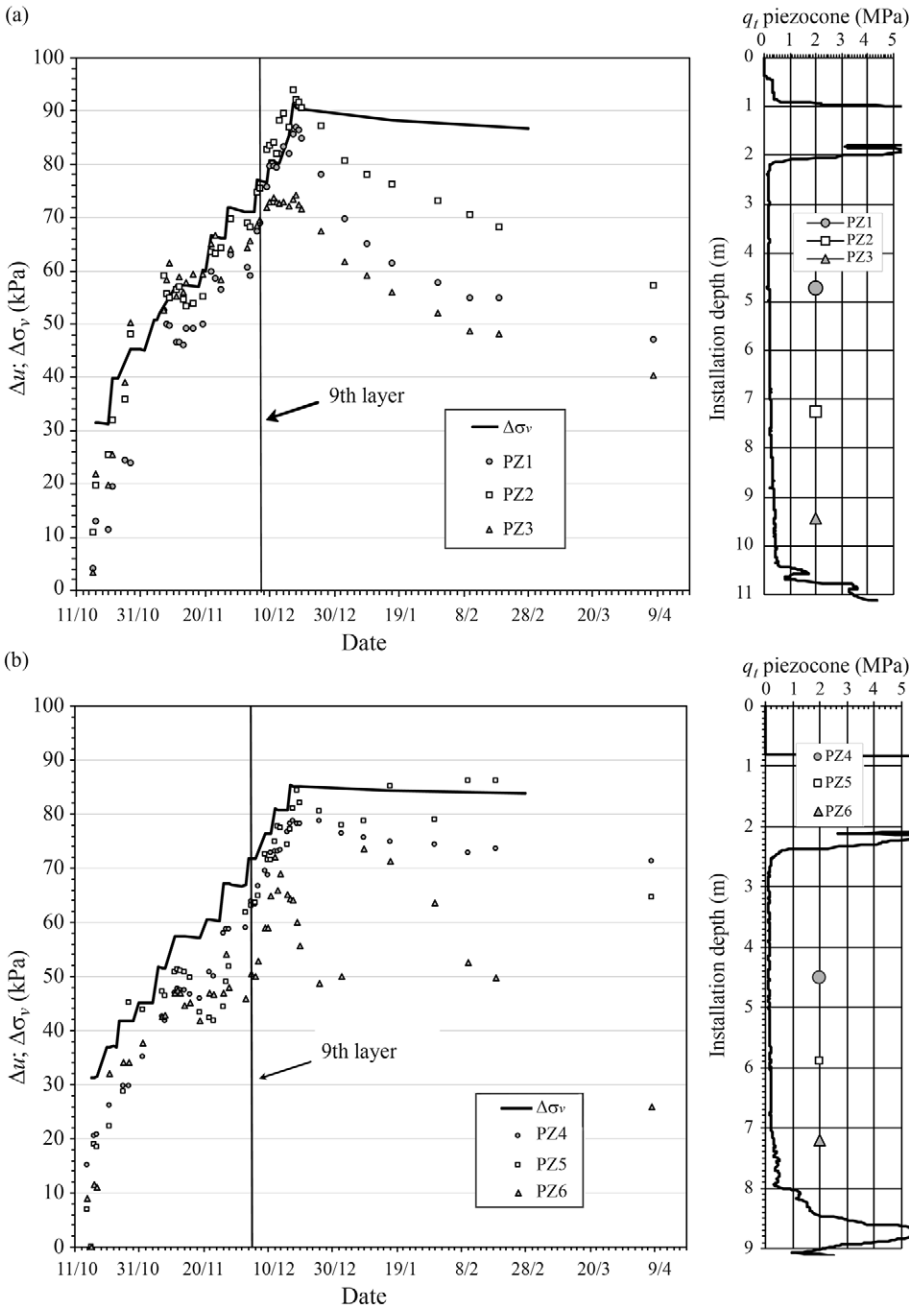

Figure 9 - Excess pore pressure and average vertical stress in clay layers: (a) embankment TE1; (b) embankment TE2.

cated on the right-hand side of Fig. 9 together with piezocone data. Values of $\Delta\sigma_v$ include the vertical stress corresponding to the surface sand layer, as consolidation was still under development. Therefore part of the measured pore pressure (generated and dissipated) was due to the placement of the surface sand layer. The vertical lines indicate the placement of the ninth layer when cracks in the embankment were observed.

The values for Δu and $\Delta\sigma_v$ shown in Fig. 9 are quite close for both embankments, *i.e.*, the ratio $\Delta u/\Delta\sigma_v$ is close to unity, an expected behaviour for normally consolidated clays, which is the present case. Values of $\Delta u/\Delta\sigma_v$ described in the literature are related to lightly over-consolidated clays and lie in the range 0.38 to 0.75 (Leroueil *et al.*, 1978), particularly at the early loading stages, owing to the relatively high value of the coefficient of consolidation of the over-consolidated soil.

The results presented in Fig. 9a suggest that the influence of the PVDs on the dissipation of pore pressures during the construction phase of embankment TE1 was apparently quite small. With regard to the post-construction phase, the data on the two piezometers near the mid-clay depth (see circles and squares in Fig. 9) show, as expected, that the pore pressures under embankment TE1 (Fig. 9a) with PVDs dissipate faster than pore pressures under embankment TE2 (Fig. 9b) without PVDs.

6. Horizontal Displacements

Three inclinometers were installed in each test embankment, one close to the embankment toe, another at the crest of the embankment and a third near the centre of the embankment, namely inclinometers I4, I5 and I6 in embankment TE2 (corresponding to I1, I2 and I3 of TE1 - Fig. 2).

Monitoring of horizontal displacements using inclinometers at the embankment toe is one of the most efficient procedures for assessing impending failure of embankments on soft clays (*e.g.*, Hunter & Fell, 2003; Magnani *et al.*, 2008). For the three embankments studied by Magnani (2006), the inclinometers located at the embankment toe showed the highest values compared with the other inclinometers. The patterns of the inclinometer measurements of the two reinforced embankments TE1 and TE2 are quite similar (Magnani, 2006). Figure 10 shows measurements of the inclinometers in the foundation layers (sand surface layer and clay layer) located at the embankment toe for reinforced test embankment TE2 and unreinforced test embankment TE3. The data shown are horizontal displacements *vs.* depth (Fig. 10a) and vertical deviation *vs.* depth (Fig. 10b). Vertical deviation or vertical inclination angle $\theta_v = \Delta\delta_h/\Delta z$ is defined by the ratio between the increment in horizontal displacements $\Delta\delta_h$ and the distance Δz between the measured points. Both curves kept their shape as embankment loading progressed, which confirms the observations of Tavenas *et al.* (1979) for unreinforced embankments on lightly over-consolidated clays. The depth at which the maximum vertical deviation value θ_{vmax} occurs remains constant during the raising of the embankment and corresponds approximately to the depth of the maximum shear strains, thus indicating the depth of the failure (*e.g.*, Hunter & Fell, 2003). The observed depths of the failure z_f are 5.0 m, 3.8 m and 1.8 m, respectively for embankments TE1, TE2 and TE3, and thus z_f increases with the increase in the thickness of the clay layer.

The depth of maximum horizontal displacements δ_{hmax} ($\theta_v = 0$) is shallower for the unreinforced embankment TE3 owing to the less thick clay layer and no reinforcement adopted.

More comprehensive data on horizontal displacements and the correlation of these with the forces measured in the reinforcement have been presented by Magnani *et al.* (2009).

7. Applied Embankment Stresses and Soft Clay Response

The response of foundation layers to the applied embankment vertical stress is shown in Fig. 11. Figure 11a shows the vertical embankment applied vertical stress $\Delta\sigma_v$ (submersion effects discounted) *vs.* the maximum vertical deviation values θ_{vmax} measured in the inclinometers located at the toe of the embankments (I1 for embankment TE1, I4 for embankment TE2 and I7 for embankment TE3). Similar results were obtained (Magnani, 2006) for the inclinometers located at the crests of the embankments.

It should be noted from Fig. 11a that the two reinforced embankments showed similar behaviour despite the fact that clay under embankment TE1 had PVDs. Figure 11a also shows that embankment TE3 reaches a higher $\Delta\sigma_v$ value than the reinforced embankments. This fact may be explained by the higher strength S_u of the clay layer (see Fig. 3), the smaller thickness of the clay layer and the presence of the sand lens within the clay layer. For these reasons, embankment TE3 cannot be considered as a reference (unreinforced) embankment in relation to the reinforced embankments TE1 and TE2.

Figure 11b shows the data of Fig. 11a normalised by the maximum applied embankment vertical stress $\Delta\sigma_{vmax}$. It is noted that curves of the three embankments get close. This is of great interest as it indicates that the shearing responses of the three clay layers were similar and, in the present case, valid for both reinforced and unreinforced embankments. Therefore, the maximum vertical deviations can be expressed solely by the failure factor of safety and by the clay strain characteristics. For a factor of safety of 1.4 ($\Delta\sigma_v/\Delta\sigma_{vmax} = 0.71$), for example, the maximum vertical deviation value θ_{vmax} for the present case is between 3% and 4% for the data contained in Fig. 11b.

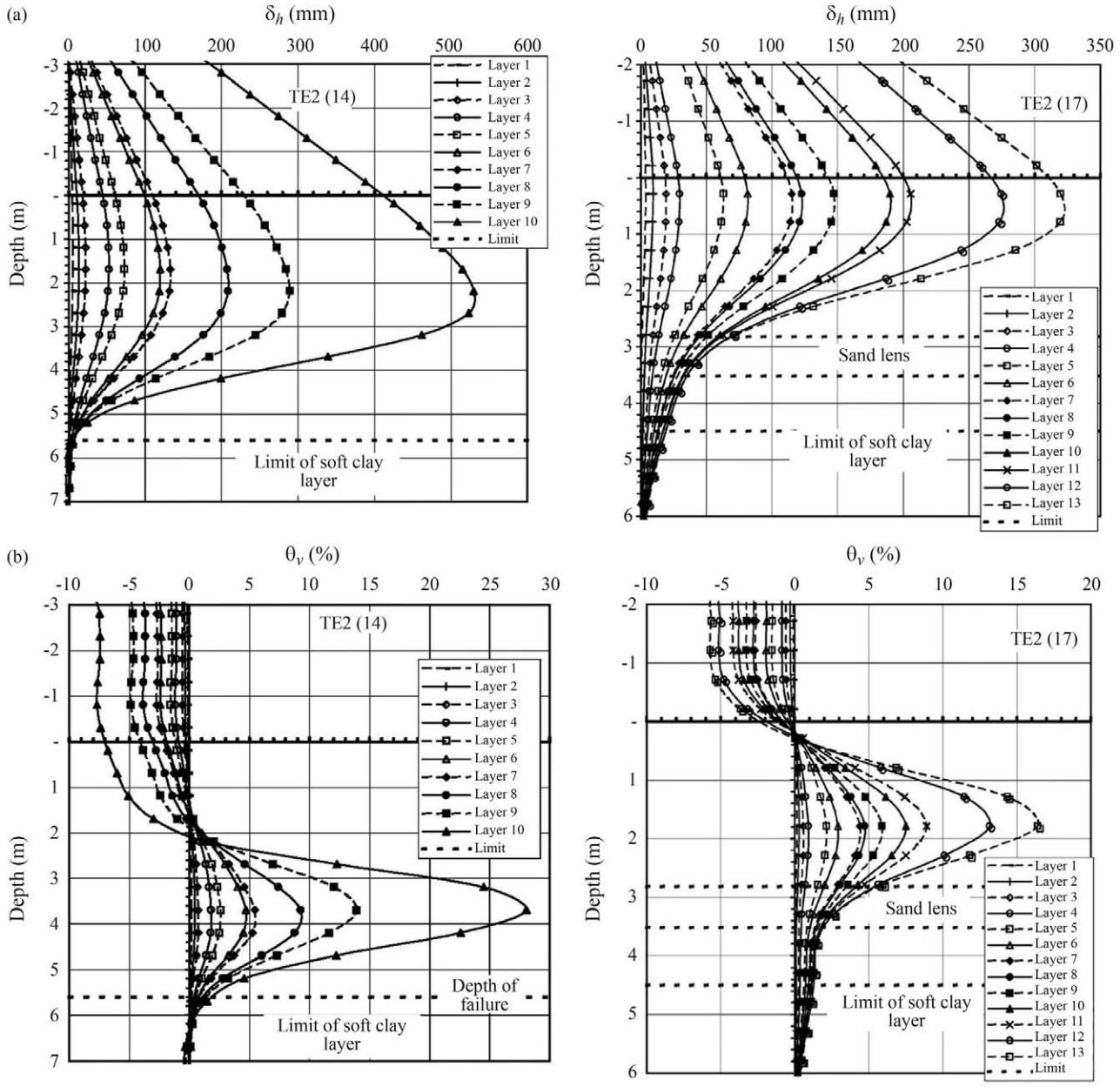

Figure 10 - Inclinometer measurements at the embankment toe: (a) horizontal displacements - δ_h; (b) vertical deviation θ_v.

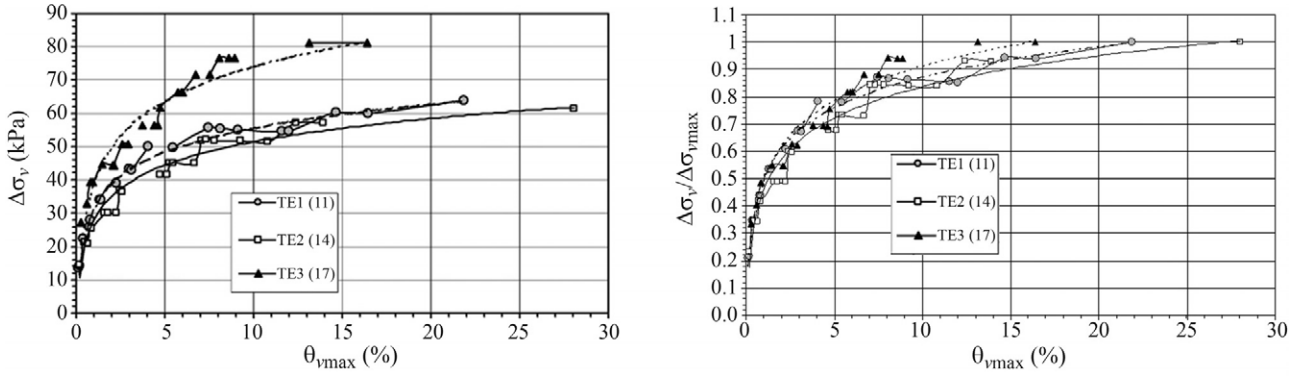

Figure 11 - Vertical embankment stress *vs.* maximum vertical deviation for inclinometers located at the toe of the embankments.

The results of Fig. 11b indicate that, despite the fact that the unreinforced embankment TE3 is a not a reference embankment in relation to the reinforced embankments TE1 and TE2, the results of the three embankments can be analysed together, thereby allowing an overall analysis of the behaviour of the clay foundation when subjected to loading. Therefore, the stability and deformation of the present test embankments on thick surface sand layers were governed by the soft clay whether the embankment was reinforced or not.

8. Stability of the Embankments

Stability analyses of the three test embankments carried out for each loading stage (Magnani *et al.*, 2009; Magnani *et al.*, 2010) produced the variation of the factor of safety *vs.* the applied vertical stress $\Delta\sigma_v$ shown in Fig. 12. These analyses were based on: (a) the measured S_u profiles shown in Fig. 2 (the small gains in strength were disregarded); (b) the measured reinforcement forces for each loading stage; (c) the Bjerrum correction factor ($\mu = 0.60$) applied to the vane strength; (d) the correction for three-dimensional effects of the failure surface (Azzouz *et al.*, 1983), which increased the conventional 2-D factors of safety by 10 to 14% depending on the test embankment; and (e) Bishop's limit equilibrium method, as the observed failure surfaces were consistent with the points of maximum vertical deviation and had circular shapes, as shown in Fig. 12 for TE2. Similar agreement was obtained for TE1 and TE3 (Magnani, 2006).

Figure 12 shows that the variation of the factors of safety F_s with applied vertical stress of embankments TE1 and TE2 are quite close. For the same applied vertical stress, unreinforced embankment TE3 shows higher factors of safety than reinforced embankments. Thus, the results shown in Fig. 12 are consistent with the stress-strain curves shown in Fig. 11a.

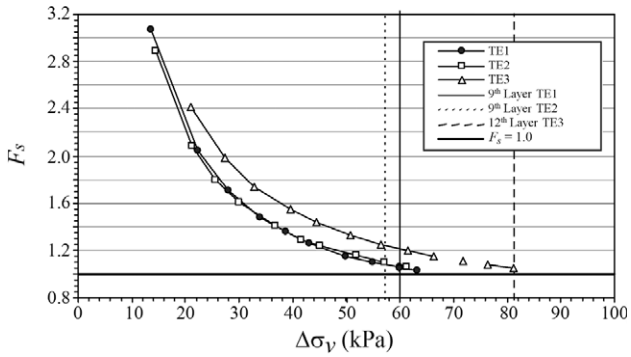

Figure 12 - Factors of safety for the three test embankments for each loading stage considering Bjerrum correction factor $\mu = 0.60$ and 3-D effects.

The overall behaviour of the three embankments can also be observed in the photos of the three embankments shown in Fig. 14. The cracks developed in embankment TE1 with PVDs and reinforcement (Fig. 14a) can hardly be seen in the picture. Embankment TE2 (Fig. 14b), also reinforced but without PVDs, developed slightly bigger cracks at the crest. The unreinforced embankment TE3 (Fig. 14c), however, presented a clear failure at the embankment crest, the step between the two platforms being around 0.70 m.

Irrespective of the fact that TE3 is not a reference embankment, since it was constructed on a thinner clay layer with higher strength and reached a higher elevation, the photos presented in Fig. 14 indicate that the use of rein-

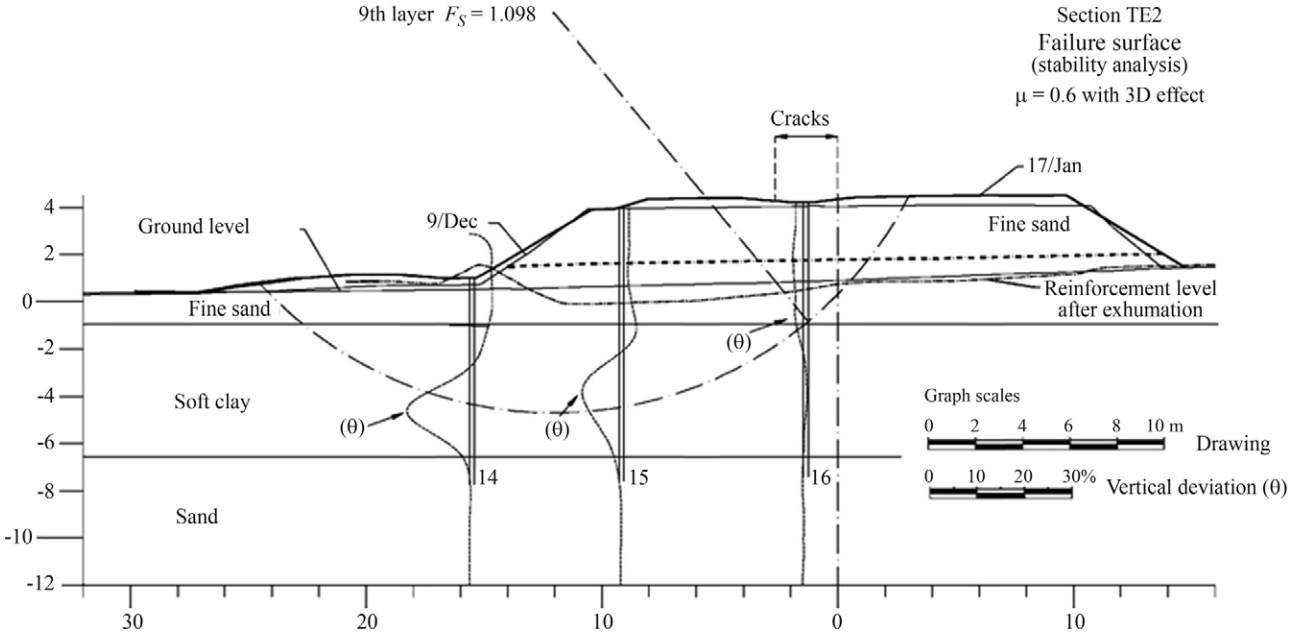

Figure 13 - Theoretical critical failure surface (stability analysis) *vs.* observed failure surface (points of maximum vertical deviation).

forcement as for embankments TE1 and TE2 resulted in better overall performance.

9. Numerical Analyses and the Relevance of PVDs

Literature recommendations (Saye, 2001) regarding PVD installation to minimize smear are drain spacing l greater than 1.50 m and a mandrel area A smaller than 65 cm^2, but values used for TE1 were l = 1.30 m and A = 180 cm^2. Therefore it appears that smear may have played an important role in the performance of test embankment TE1. Therefore, numerical 2-D finite element analyses of TE1 were carried out using the Plaxis program (Brinkgreve, 2010) to assess the importance of the PVDs in this test embankment loaded quickly to failure.

Figure 14 - Photos of the crest of the test embankments at failure.

9.1. Material parameters

For these analyses elasto-plastic soil models available in the Plaxis program were used; the *Soft Soil model,* a Cam-clay type model for the soft clay and the *Hardening Soil model* for the sand materials (embankment and sand fill). Parameters for sand layers and soft clay are presented in Tables 3 and 4, respectively.

The geosynthetic reinforcement was modelled as an elastic material with stiffness J = 1,700 kN/m with 15-node soil finite elements adopted for this 2-D analysis. The geosynthetic layer was modelled using structural finite elements.

9.2. Modelling of PVDs in FE analysis

For test embankment TE1 provided with PVDs, an equivalent 2-D plane strain multi-drain analysis (Indraratna & Redana, 2000; Indraratna, 2009) was carried out.

To perform a multidrain analysis, it is necessary to adopt a coefficient of horizontal permeability for plane strain conditions $k_{h,ps}$ different from the horizontal coefficient of permeability used for axi-symmetric unit cell conditions $k_{h,ax}$. This correspondence uses geometric data and may also assume drain smear as explained below.

Table 3 - Parameters for sand materials – Hardening Soil model.

Parameter	Value
Effective friction angle	35°
Dilatance angle	0°
Effective cohesion (kPa)	0 (*)
Stiffness Modulus $E_{50}^{ref} = E_{oed}^{ref}$ (kN/m^2)	18,000
Stiffness Modulus E_{ur}^{ref} (kN/m^2)	52,000
Poisson ratio	0.3
Bulk weight (kN/m^3)	17.5

(*) for the unsaturated embankment c = 1 kPa was adopted.

Table 4 - Parameters for the soft clay layer – Soft Soil model.

Parameter	Value
Effective friction angle (°)	30
Effective cohesion (kPa)	5.0
$C_c/(1 + e_o)$	0.36
$C_s/(1 + e_o)$	0.039
Over-consolidation ratio – OCR	1.1
Ko	0.53
Bulk weight (kN/m^3)	13.7

As far as drain smear is concerned, a typical literature value equal to 3.0 was adopted for the ratio $k_{h,ax}/k_{s,ax}$ between the coefficient of horizontal permeability in the intact soil ($k_{h,ax}$) and the smeared soil ($k_{s,ax}$).The equivalent coefficient of horizontal permeability in plane strain $k_{h,ps}$ and the equivalent horizontal permeability to the smear zone $k_{s,ps}$ can be computed based on the horizontal soil intrinsic coefficient of horizontal permeability $k_{h,ax}$ and geometric data using the equations (Indraratna & Redana, 2000).

$$\frac{k_{h,ps}}{k_{h,ax}} = \frac{\frac{2}{3}\left[\frac{(n-1)^2}{n^2}\right]}{\left[\ln(n) - \frac{3}{4}\right]} \quad (2)$$

$$\frac{k_{s,ps}}{k_{h,ps}} = \frac{\beta}{\frac{k_{h,ps}}{k_{h,ax}}\left[\ln\left(\frac{n}{s}\right) + \frac{k_{h,ax}}{k_{s,ax}} - \frac{3}{4}\right] - \alpha} \quad (3)$$

$$\alpha = \frac{2}{3}\frac{(n-s)^3}{n^2(n-1)} \quad (4)$$

$$\beta = \frac{2(s-1)}{n^2(n-1)}\left[n(n-s-1) + \frac{1}{3}(s^2+s+1)\right] \quad (5)$$

where $n = d_e/d_w$ is the ratio of the diameter of the unit cell d_e to the equivalent drain diameter d_w and $s = d_s/d_w$ relates the diameter of the smear zone d_s with d_w.

For the triangular drain mesh spaced 1.3 m d_e = 1.3 x 1.05 = 1.365 m. Considering PVD dimensions a = 10 cm and b = 0.5 cm, then $d_w = 2(a + b)/\pi = 0.067$ m. Therefore, $n = d_e/d_w = 20.42$ m.

The diameter of the smear zone d_s is assumed equal to 2.5 times the equivalent mandrel diameter d_m which in turn is a function of the adopted mandrel area equal to 180 cm^2, thus $d_m = (0.018*4/\pi)^{0.5} = 0.0874$ m and d_s = 2.5 x d_m = 0.22 m, and $s = d_s/d_w = 3.27$ m.

The adopted value of the vertical coefficient of permeability k_v was 10^{-9} m/s. Then, if we assume isotropy in terms of the horizontal coefficient of permeability of the intact soil is $k_{h,ax} = 10^{-9}$ m/s. As $k_{s,ax}/k_{h,ax} = 3$, then the horizontal coefficient of permeability of the smeared soil is $k_{s,ax}$ = 3.33 x10^{-10} m/s. Then, substituting these values and the values of n and s obtained above into Eqs. (2) to (5), one obtains for the intact soil $k_{h,ps}$ = 2.66 x10^{-10} m/s and for the smeared zone $k_{s,ps}$ = 0.71 x10^{-10} m/s, which were the values used in the plane strain finite element analyses.

9.3. Numerical results *vs.* measured data

Three finite element analyses were carried out for test embankment TE1: (a) "PVD" which is expected to be the condition closest to the actual conditions of test embankment TE1; (b) "PVD no-smear" assuming that PVDs installation caused no smear, to compare this with "PVD analysis" in which smear is considered; (c) "no-PVD" for a virtual condition for TE1 without PVDs, to assess the influence of the PVDs. The main features of these analyses are summarized in Table 5, which also presents the values of vertical and horizontal coefficients of permeability adopted in these 2-D FE analyses.

The PVDs multi-drain analysis (Indraratna & Redana, 2000) assumes the width of the unit cell in plane strain conditions to be the same as the diameter d_e of the axi-symmetric unit cell. It also assumes that the drain width in plane strain is equal to the equivalent drain diameter d_w and similarly with respect to the smear zone. The finite element mesh adopted following these features is shown in Fig. 15 for the "PVD analysis" and "PVD no-smear analysis" (around 19,000 elements). The "no PVD analysis" used a similar FE mesh (around 8400 elements), obviously without PVDs.

The actual TE1 test embankment loading history was adopted for the three analyses, thus consolidation was allowed during the whole period of about two months of embankment construction, during both loading and waiting periods between each layer placement.

Computed and measured settlements, with and without PVDs, for the settlement plate PB7 (see Fig. 2) are shown in Fig. 16 for the three analyses. Good overall agreement between measured and "PVD analysis" is observed, which suggests that the multidrain analysis and the adopted

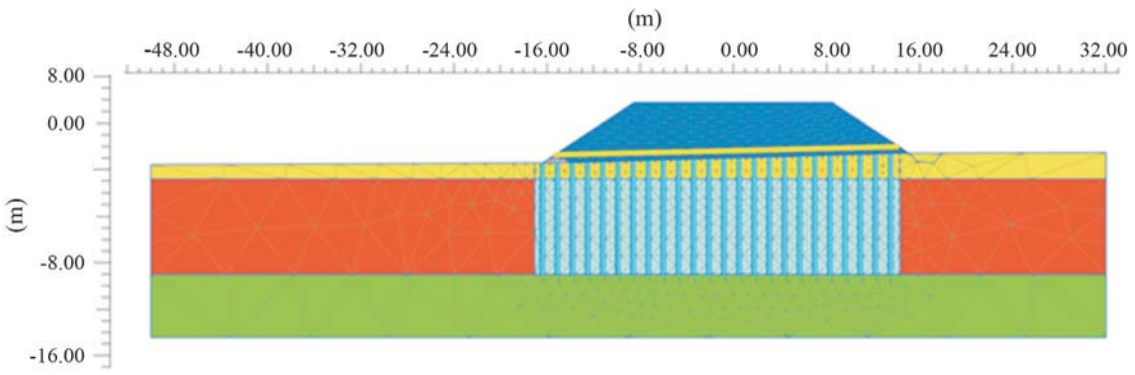

Figure 15 - Finite element mesh adopted for the PVD analyses.

Table 5 - Main features of the 2D multidrain FE analyses performed.

Analysis	PVDs	smear	Region	k_v (10^{-10} m/s)	k_h (10^{-10} m/s)
"PVD"	yes	yes	Drain region (smear)	3.33	0.71
			Drain region	10	2.66
			Outside the drain region	10	10.0
"PVD no-smear"	yes	no	Drain region	10	2.66
			Outside the drain region	10	10
"no-PVD"	no	-	-	10	10

model parameters are adequate. Agreement is quite good until 20 November, but for subsequent times the numerical analysis slightly under-predicts measured settlements.

Figure 16 shows also that settlements of "no-PVD analysis" are smaller than settlements of "PVD analysis" (and measured settlements), thus showing that PVDs had a beneficial effect in accelerating settlements. The influence of smear is also noticed in Fig. 16 by comparing results of "PVD analysis" and "PVD no-smear analysis", the latter presenting larger settlements, as expected.

The three time-settlement curves showed a change in slope, indicating large yield zones and the start of the failure process. The time corresponding to these changes in slope roughly coincides with the time of the actual failure process in test embankment TE1 (layers 9 and 10). It may be observed that this time for the "no PVD analysis" starts slightly earlier than for the two PVD analyses. It may also be observed that FE analysis could not continue much further due to lack of numerical convergence.

Results of computed and measured maximum horizontal displacement are shown in Fig. 17 for the inclinometer I1 located at the embankment toe. It is observed that the computed values are quite close to and slightly larger than the measured values until 10 November. Better agreement is observed for intermediate times, particularly for the "PVD analysis".

For dates after 10 November, differences between the numerical analyses increase. The differences between these analyses follow the same trend observed for vertical displacements, with displacements becoming larger as drainage conditions improve, *i.e.*, smaller horizontal displacements for "no-PVD analysis" which increase for the "PVD analysis" and increase further for the "PVD no-smear analysis".

Results of the computed and measured total pore pressures for piezometer PZ1 are shown in Fig. 18. The measured results increase continuously with time with negligible pore pressure dissipation. A similar pattern is observed for "PVD analysis" which also compares well with the measured results, suggesting that smear was well simulated in this multidrain analysis. Results of "PVD no-smear analysis", also shown in Fig. 18, are close to "PVD analysis" up to 20 November and then show smaller values.

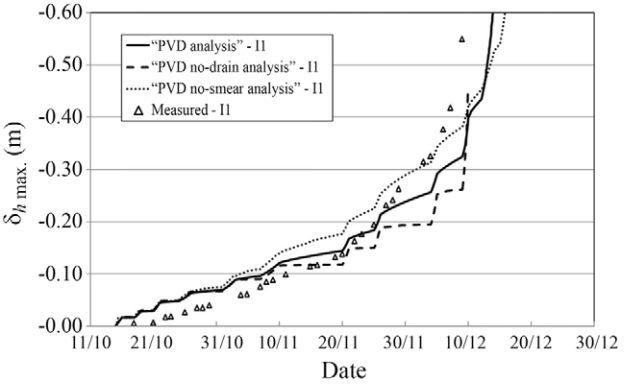

Figure 17 - FE results x field measurements – Maximum horizontal displacement (I1).

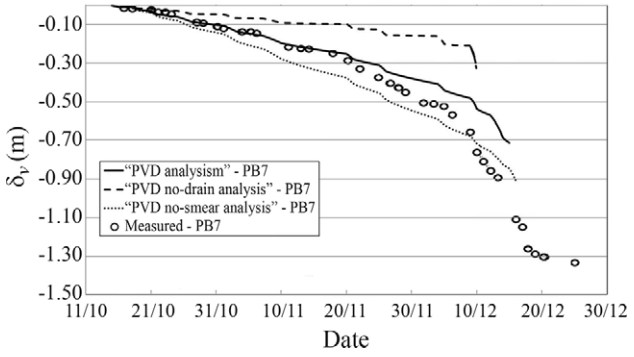

Figure 16 - FE results x field measurements – Vertical displacement (PB7).

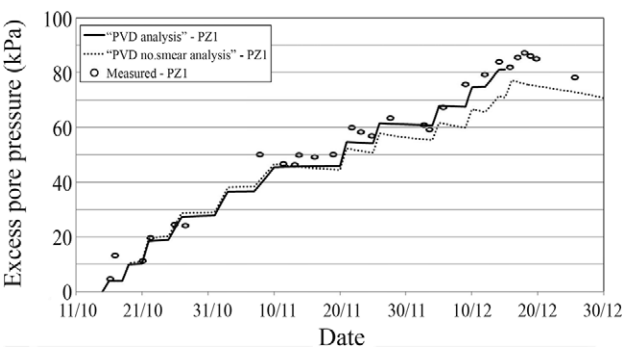

Figure 18 - FE results x field measurements – Excess of pore pressure for PZ1.

These results show more pronounced pore pressure dissipation following loading, thus indicating better drain performance when no smear occurs, as expected.

Overall assessment of the numerical analyses shows that PVDs influenced the performance of TE1 but this influence appears to be smaller than shown in the literature (*e.g.*, Li & Rowe, 2001). The reasons for this appear to be the very low value of the coefficient of consolidation of Florianopolis clay, disturbance effects due to drain installation and the short construction time.

10. Conclusions

Three test embankments (two reinforced and one unreinforced) were rapidly constructed to failure on normally consolidated clay layers overlain by pre-constructed surface sand layers. The foundation of one of the reinforced embankments (TE1) was provided with PVDs.

The embankment without reinforcement and PVDs (TE3) reached a higher vertical stress (or net embankment height) at failure than the two reinforced embankments owing to its greater clay strength. The two reinforced embankments (TE1 and TE2) presented similar maximum vertical stress at failure. This was because of the similarity in the undrained strength values of the two clay layers. Owing to the low coefficient of consolidation of the normally consolidated clay, the rapid construction of the test embankments and drain disturbance (close drain spacing and large mandrel used) the PVDs had, in the present case, a relatively small effect on the behaviour of the reinforced embankment provided with vertical drains. These conclusions are supported by the results obtained by finite element analyses. Numerical analyses showed that the PVD had a greater influence on settlement and on horizontal displacements than on pore pressure results and that smear appears to play an important role in this particular case history.

The curves of variation of factors of safety *vs.* applied embankment stress showed very close values for reinforced embankments TE1 and TE2 and higher factors of safety in general were obtained for unreinforced embankment TE3.

The normalisation of the applied embankment stress by the maximum applied stress *vs.* the clay shearing strains produced close stress-strain curves for the three embankments. Thus the responses of the embankments to the normalised embankment stresses are independent of the thickness of the soft layer and are valid, in the present case, for both reinforced and unreinforced embankments.

The photos of the failures show that the reinforcement was effective in controlling large cracks at failure, and the unreinforced embankment presented a clear failure surface with a step at the crest of the embankment.

Acknowledgments

The authors are indebted to all the individuals and institutions that made the construction of the three test embankments possible, in particular the technical staff of COPPE-UFRJ Geotechnical Laboratory for the installation of the instruments. Maria Cascão, Politechnic School, Federal University of Rio de Janeiro presented important suggestions for the development of the finite element analyses.

References

Almeida, M.S.S.; Britto, A.M. & Parry, R.H.G. (1986) Numerical modeling of a centrifuged embankment on soft clay. Canadian Geotechnical Journal, v. 23:2, p. 103-114.

Almeida, M.S.S.; Davies, M.C.R. & Parry, R.H.G. (1985) Centrifuge tests of embankments on strengthened and unstrengthened clay foundations. Géotechnique, v. 35:4, p. 425-441.

Almeida, M.S.S.; Futai, M.M.; Lacerda, W.L. & Marques, M.E.S. (2008) Laboratory behaviour of Rio de Janeiro soft clays. Part 1: Index and compression properties. Soils and Rocks, v. 31:2, p. 69-75.

Almeida, M.S.S. & Marques, M.E.S. (2002) The behaviour of Sarapuí soft clay. Proceedings of the International Workshop on Characterization and Engineering Properties of Natural Soils, v. 1, pp. 477-504, Balkema, Singapore.

Almeida, M.S.S.; Marques, M.E.S. & Spotti, A.P. (2005) Two case histories of vertical drains in very soft clays. Buddhima, I.; Chu, J. & Hudson, J.A. (eds) Ground Improvement - Case Histories. Geo-Engineering Book Series, Elsevier, chap 5, pp. 145-157

Almeida, M.S.S.; Spotti, A.P.; Santa Maria, P.E.L.; Martins, I.S.M. & Coelho, L.B.M. (2001) Consolidation of a very soft clay with vertical drains. Geotechnique, v. 50:2, p. 633-643.

Almeida, M.S.S.; Ehrlich, M.; Riccio, M.; Magnani, H. & Souza, H. (2010) Development and performance of load cell systems for reinforced embankment and reinforced soil wall. Proceedings 9th International Conference on Geosynthetics, Guarujá, Brazil, v. 4, p. 1869-1874.

Azzouz, A.S.; Baligh, M.M. & Ladd, C.C. (1983) Corrected field vane strength for embankment design. Journal of Geotechnical Engineering ASCE, v. 109:5, p. 730-735.

Bergado, D.T.; Chai, J.; Alfaro, M.C. & Balasubramanian, A.S. (1994) Improvement Techniques of Soft Ground in Subsiding and Lowland Environment. Balkema, Rotterdam, 232 pp.

Brinkgreve, R.B.J. (2010). PLAXIS – 2D User's Manual. Rotterdam, Netherlands, 682 pp.

Chai, J.; Miura, N. & Shen, S. (2002) Performance of embankments with and without reinforcement on soft subsoil. Canadian Geotechnical Journal, v. 39:4, p. 838-848.

Dunnicliff, J. (1988) Geotechnical Instrumentation for Monitoring Field Performance. John Wiley, New York, 608 p.

Hinchberger, S. & Rowe, R.K. (2003) Geosynthetic reinforced embankments on soft clay foundations predicting reinforcement strain at failure. Geotextiles and Geomembranes, v. 21:3, p. 151-175.

Holtz, R.D. (1987) Preloading with prefabricated vertical strip drains. Geotextiles and Geomembranes, v. 6:1-3, p. 109-131.

Humphrey, D.N. & Holtz, R.D. (1989) Effect of surface crust on reinforced embankment. Proceedings of Geosynthetics '89, Industrial Fabrics Association International, St, Paul, v. 1, pp. 136-147.

Hunter, G. & Fell, R. (2003) Prediction of impending failure of embankments on soft ground. Canadian Geotechnical Journal, v. 40:1, p. 209-220.

Indraratna, B.; Balasubramaniam, A.S. & Balachandran, S. (1992) Performance of test embankment constructed to failure on soft marine clay. Journal of Geotechnical Engineering, ASCE, v. 118:1, p. 12-33.

Indraratna, B. & Redana I.W. (2000) Numerical modeling of vertical drains with smear and well resistance installed in soft clay. Canadian Geotechnical Journal, v. 37:1, p. 133-145.

Indraratna, B. (2009) "Recent advances in the application of vertical drains and vacuum preloading in soft soil stabilization", 2009 EH Davis Memorial Lecture – Australian Geomechanics Journal, v. 45, p.603-617.

Kelln, C.; Sharma, J.; Hughes, D. & Gallagher, G. (2007) Deformation of a soft estuarine deposit under a geotextile reinforced embankment. Canadian Geotechnical Journal, v. 44:5, p. 603-617.

Leroueil, S.; Tavenas, F.; Mieussens, C. & Peignaud, M. (1978) Construction pore pressures in clay foundations under embankments. Part II: Generalized behaviour. Canadian Geotechnical Journal, v. 15:1, p. 65-82.

Li, A.L. & Rowe, R.K. (2001) Combined effects of reinforcement and prefabricated vertical drains on embankment performance.Canadian Geotechnical Journal, v. 38:6, p. 1266-1282.

Lo, S.R.; Mak, J.; Gnanendran, C.T.; Zhang, R. & Manivannan, G. (2008) Long-term performance of a wide embankment on soft clay improved with prefabricated vertical drains. Canadian Geotechnical Journal, v. 45:8, p. 1073-1091.

Magnani, H. (2006) Comportamento de Aterros Reforçados Sobre Solos Moles Levados a Ruptura. Tese D.Sc, Programa de Engenharia Civil, COPPE/UFRJ, Rio de Janeiro.

Magnani, H.O.; Almeida, M.S.S. & Ehrlich, M. (2008) Construction stability evaluation of reinforced embankments over soft soils. Proceedings of First Pan American Geosynthetics Conference & Exhibition, March 2008, Cancun, CD-Rom.

Magnani, H.O.; Almeida, M.S.S. & Ehrlich, M. (2009a) Behaviour of two reinforced test embankments on soft clay taken to failure. Geosynthetics International, v. 16:3, p. 127-138.

Magnani, H.O.; Ehrlich, M. & Almeida, M.S.S. (2009b) Embankments over soft clay deposits: the contribution of basal reinforcement and surface sand layer to stability. Journal of Geotechnical and Geoenvironmental Engineering ASCE, v. 136, p. 260-265.

Massad, F. (1994) Propriedades dos sedimentos marinhos. In: Solos do Litoral Paulista. Associação Brasileira de Mecânica dos Solos, São Paulo, pp. 99-128.

Pinto, C.S. (1994) Aterros na baixada, In: Solos do Litoral Paulista. Associação Brasileira de Mecânica dos Solos, São Paulo, pp. 235-264.

Rowe, R.K.; Gnanendran, C.T.; Landva, A.O. & Valsangkar, A.J. (1995) Construction and performance of a full-scale geotextile reinforced test embankment, Sackville, New Brunswick. Canadian Geotechnical Journal, v. 32:3 p. 512-534.

Rowe, R.K.; Gnanendran, C.T.; Landva, A.O. & Valsangkar, A.J. (1996) Calculated and observed behaviour of a reinforced embankment over soft compressible soil. Canadian Geotechnical Journal, v. 33:2, p. 324-338.

Rowe, R.K. & Leroueil, S. (2001) Embankments over soft soil and peat. Rowe, R.K. (ed), Geotechnical and Geoenvironmental Engineering Handbook. Kluwer, Norwell, pp. 463-499.

Rowe, R.K. & Li, L.L. (2005) Geosynthetic-reinforced embankments over soft foundations. Geosynthetics International, v. 12:1, p. 50-85.

Rowe, R.K. & Soderman, K.L. (1987b) Reinforcement of embankments on soils whose strength increases with depth. Proceedings of the Geosynthetics '87 Conference, New Orleans, pp. 266-277.

Saye, S.R. (2001) Assessment of soil disturbance by the installation of displacement sand drains and prefabricated vertical drains. Proceedings of Symposium on Soil Behaviour and Soft Ground Construction, Geotechnical Special Publication no. 119. Geo-Institute ASCE, Cambridge, pp. 325-362.

Schnaid, F. (2009) In Situ Testing in Geomechanics. Taylor and Francis, Oxon, 352 pp.

Tavenas, F.; Mieussens, B. & Bourges, F. (1979) Lateral displacements in clay foundations under embankments. Canadian Geotechnical Journal, v. 16:3, p. 532-550.

Zhang, L. (1999) Settlement patterns of soft soil foundations under embankments. Canadian Geotechnical Journal, v. 36:4, p. 774-781.

List of Symbols

c = cohesion (kPa)
C_c = compression index
C_s = swelling index
c_v = coefficient of vertical consolidation (m/s^2)
e = void ratio (dimensionless)
F_s = factor of safety (dimensionless)

G = shear modulus (kPa)
h = embankment height (m)
h^* = embankment thickness less measured settlement (m)
I_P = plasticity index (%)
J = reinforcement modulus = T/ε_a (kN/m)
N_{kt} = empirical cone factor (dimensionless)
q_T = corrected point resistance (kPa)
S_u = undrained clay strength (kPa)
z = depth (m)
z_f = depth of the failure (m)
w = water content (%)
w_L = liquidity index (%)
δ_h = horizontal displacement (m)
δ_v = vertical displacement (m)
ε_a = reinforcement strain (%)
Δu = excess pore pressure (kPa)
$\Delta\sigma_v$ = applied embankment vertical stress (kPa)
$\Delta\sigma_{vmax}$ = maximum applied (submersion effects discounted) embankment vertical stress (kPa)
ϕ = friction angle (°)
γ = bulk weight (kN/m^3)
μ = Bjerrum correction factor (dimensionless)
θ_v = vertical deviation (dimensionless)
θ_{vmax} = maximum vertical deviation (dimensionless)
σ_v = total vertical stress (kPa)
$k_{h,ps}$ = equivalent coefficient of horizontal permeability in plane strain (m/s)
$k_{s,ps}$ = equivalent coefficient of horizontal permeability to the smear zone in plane strain (m/s)
$k_{h,ax}$ = coefficient of horizontal permeability (m/s)
k_v = vertical coefficient of permeability